IRANIAN JOURNAL OF PHYSICS RESEARCH

Iranian Journal of Physics Research, Vol. 5, No. 2, 2005

Zr/Ba/Na fluoride glass molecular dynamics studies at atmospheric pressure and 4 GPa I: equilibration and the glass transition

S Gruenhut[1], M Amini[2*], D R MacFarlane[1] and P Meakin[1]

1.Department of Chemistry, Monash University,
Clayton, Melbourne, 3168, Australia

2.Department of Physics, Isfahan University
of Technology, Isfahan, Iran
E-mail: m_amini@cc.iut.ac.ir

(Received 26 December 2004; accepted 18 January 2005)

Abstract

A constant volume, atmospheric pressure Zr/Ba/Na fluoride glass has been simulated by molecular dynamics with the limitations of the Born-Mayer-Huggins potentials, used previously and resulting in high simulation pressures, having been overcome. The simulated structure of this glass as well as its activation energy for diffusion are in very good agreement with those experimentally observed. To highlight the changes brought on by the decrease in pressure, the simulation at atmospheric pressure has been compared with one at high pressure. The results show that structural energy (total and potential), specific heat and pressure derivative changes occur with the reduction in pressure. In addition, a greater structural relaxation rate and a glass with a lower configurational variation were also observed. The glass transition has also been studied and it was found, on moving from glass to liquid temperatures, to be caused by the breaking of structural and geometric constraints. As expected, a sharp increase in the MSD was observed after the glass transition.

Keywords: molecular dynamics, equilibration, glass transition, atmospheric Pressure, fluoride glasses, ZBN

1. Introduction

Many molecular dynamics studies have attempted to simulate the physical properties of Zr/Ba/Na fluoride glass. However, limitations in the Born-Mayer-Huggins (BMH) interparticle potential have resulted in high simulation pressures, (of the order of 4 GPa), or low simulation densities [1-5] consequently the physical properties derived from these simulations are not accurate. This study reports the molecular dynamics simulation of Zr/Ba/Na fluoride glass (57 mole % ZrF_4: 21.5 mole % BaF_2: 21.5 mole % NaF) with atmospheric pressure being achieved at room temperature and at a physical density. Also discussed is the method by which the limitations of the BMH potential were overcome.

The glass transition, as observed experimentally, is a kinetic phenomenon which depends on the time scale of observation[6]. It occurs when the relaxation towards a metastable liquid equilibrium takes longer than the period of observation[7, 8]. Previous molecular dynamics studies of the glass transition in silicates and other systems have probed structural (radial distribution functions and structure factor), thermodynamic (total energy, potential energy, enthalpy, C_p, C_v and density), and ionic motion (diffusion and individual ion motion) changes across the glass transition, under both constant volume and constant pressure conditions [9-19]. An example of an early study of the glass transition by molecular dynamics is that of Woodcock, Angell and Cheeseman who studied the glass transition in KCl and $ZnCl_2$ under constant pressure (temperature variable) and constant temperature (pressure variable) simulations using a Born-Mayer-Huggins pair potential [9]. They found abrupt changes in the derivatives of the volume versus temperature and enthalpy versus temperature curves at 348 K. These abrupt changes are characteristic of an experimental glass transition. The ionic diffusion

* Corresponding Author

rates were also found to vanish at the glass transition. Comparing the simulation results with the experimental results, Woodcock et al. found that the change in C_p between the simulated liquid and glass (C_p(liq)/C_p(glass)=1.3) was of the same magnitude as that obtained experimentally for ionic glasses (1.2-1.8). Examining the glass transition in KCl by holding the temperature constant and increasing the pressure (starting volume was 50 cm^3 $mole^{-1}$) caused the diffusivity to decrease linearly with volume and then vanish at 36.2 cm^3 $mole^{-1}$, the glass transition. The pressure dependence of the glass transition was found to be comparable to experimental values for simple ionic systems (mixed calcium + potassium nitrates and small organic chlorides). The simulations of $ZnCl_2$ also showed a glass transition but, as expected, at a much higher temperature 650 K, when compared with the experimental value of 380 K. They also found that the activation energies for diffusion of Zn^{++} and Cl^- were only 30% of their constant pressure quantities.

Another study of the glass transition by molecular dynamics is that of Valle and Andersen[14]. Pure silica was simulated using a constant volume molecular dynamics simulation with a physical density of 2.20 g/cm^3 (glassy silica). An ionic pair potential, similar in form to the Buckingham potential, was used with the parameters taken from the literature. The structure at 300 K was in satisfactory agreement with experimental data, with the density being 5% too high. Calculation of the simulated specific heats for liquid and glassy silica showed that these were in agreement with experimental values. However, no abrupt change in the gradient of the total energy, specific heat, was observed at the glass transition. This correlates with experimental observations, as silica is one of the few compounds which does not show an observable discontinuity in the specific heat at the glass transition. The glass transition temperature was observed as a step in the potential energy of minimised snapshots (to remove thermal 'noise') against temperature. As above, the simulated glass transition temperature of 2200 K was much higher than the experimental temperature of 1446 K. The diffusion coefficients of silicon and oxygen ions were also monitored as a function of temperature. These showed that the diffusion rates of the ions tended to zero at the glass transition. The activation energies for the diffusion coefficients were only 50% of the experimental value. Valle and Andersen proposed that since the viscosity is very sensitive to volume and since the simulation was at a constant volume (experimental values being obtained at constant pressure) this might explain part of the discrepancy.

The glass transition in LiCl and $(LiCl)_{0.50}(KCl)_{0.40}(CsCl)_{0.10}$ was studied by Kinugawa using constant pressure molecular dynamics again with a Born-Mayer-Huggins ionic pair potential[18]. The density of LiCl at 1200 K was within 3% of the physical density. The two simulations were then cooled to 300 K. The derivatives of volume versus temperature and enthalpy versus temperature showed an abrupt change at 600 K which is a direct indication of the glass transition. In the case of $(LiCl)_{0.50}(KCl)_{0.40}(CsCl)_{0.10}$ the simulated glass transition temperature was almost double the experimental value of 347 K. The enthalpy and volume curves remained linear from T_g to $2T_g$.

In summary, these three examples have shown that the glass transition can be simulated by molecular dynamics in the canonical ensemble, but that it usually occurs at a much higher temperature and over a broader temperature range when compared with experimental results [9-19].

In this work, the nature of the glass transition has been examined and compared in terms of structure, energy, specific heat, ionic diffusion and pressure for two simulated canonical ensemble, physical density, systems. For the first time, after extensive potential parameter investigations, an atmospheric pressure glass at room temperature was achieved, *system A*. This system was compared against a simulation run in the normal way resulting in a high pressure (4 GPa) glass at room temperature, *System B*[1].

2. Computational method

Simulating a glass using molecular dynamics involves selecting a potential and tuning its parameters, equilibration of the liquid at a high temperature, quenching, data sampling and analysis[20]. In this work, the Buckingham potential was used initially with its dispersion terms neglected for simplicity [2, 21]. It is functionally and mathematically equivalent to the Born-Mayer-Huggins (BMH) potential commonly used in the fluoride glass field (i.e. BMH with dispersion terms neglected) but it is easier to tune as it has fewer parameters. The Buckingham potential is given by:

$$U_{ij} = \frac{-q_i q_j}{4\pi\varepsilon_\circ r_{ij}} + A_{ij} \exp\left[\frac{-r_{ij}}{\rho_{ij}}\right] - \frac{C_{ij}}{r_{ij}^6} \quad , \qquad (1)$$

where q_i and q_j are the charges of the individual ions i and j, r_{ij} is the distance between the ions, $\varepsilon_\circ$ is the permittivity of free space, A_{ij} is a constant and ρ_{ij} is the hardness parameter [22]. The parameter, C_{ij}, represents dipole-dipole dispersion. In common with previous fluoride glass simulations [1-5], the Buckingham potential simulations resulted in pressures of the order of 4 GPa.

The BMH potential was chosen for *system A* as it gave greater flexibility in the adjustment of the potential parameters. The BMH pair potential has the form:

1. To the authors' knowledge no previous molecular dynamics studies of the glass transition in Zr/Ba/Na based fluoride glasses have been conducted.

Table 1. Buckingham Potential Parameters used for *system B* .

Pair Function	A_{ij} / eV	ρ / Å
Ba-Ba	100000	0.29
Ba-Na	100000	0.29
Ba-F	3500.8	0.29
Ba-Zr	35000	0.29
Na-Na	5000	0.29
Na-F	600	0.29
Na-Zr	117.6	0.29
F - F	1000	0.29
F -Zr	1800	0.29
Zr-Zr	77.8	0.29

Table 2. BMH Potential Parameters used in the simulation of *system A* .

Pair Function	$A_{ij}*b$ / eV	$\sigma_i + \sigma_j$ / Å	ρ / Å	C_{ij} / eV	m
Ba-Ba	5.58353	2.84	0.29	0	0
Ba-Na	88.8097	2.04	0.29	0	0
Ba-F	0.26660	2.75	0.29	0	0
Ba-Zr	14.440	2.26	0.29	0	0
Na-Na	0.4405	2.04	0.29	0	0
Na-F	0.1815	2.35	0.29	0	0
Na-Zr	0.1927	1.86	0.29	0	0
F - F	0.1039	2.66	0.29	0.07415	1
F -Zr	1.0129	2.17	0.29	0	0
Zr-Zr	0.237	1.68	0.29	0	0

$$U_{ij} = \frac{q_i q_j}{4\pi\varepsilon_\circ r_{ij}} + A_{ij}^{BMH}.b.\exp\left[\frac{\sigma_i + \sigma_j}{\rho}\right].\exp\left[\frac{-r_{ij}}{\rho}\right] - \frac{C_{ij}}{r_{ij}^m} - \frac{D_{ij}}{r_{ij}^n}, \quad (2)$$

where A_{ij}^{BMH} is the Pauling factor (a function of the ionic charge) and σ_i and σ_j are the characteristic ionic radii. The Born repulsive parameters are ρ and b (b is an arbitrary constant). The C_{ij} and D_{ij} terms represent the dipole-dipole and dipole-quadrapole dispersion respectively, with n and m typically having values of 6 and 8.

The parameters for both the Buckingham and BMH potentials were tuned by initially selecting a suitable X-ray pattern of a Zr/Ba/Na crystal, $BaNaZr_2F_{11}$[23-25]. The crystal structure was then convolved with Gaussian distributions, defined by the anisotropic temperature factors, to produce pair distribution functions (PDFs) for the crystal structure at room temperature. The initial potential term values were set as per Lucas et al.[2]. In this method, the hardness parameter for all ions, as well as the fluoride size parameter, are fixed. The other size parameters are then empirically chosen such that the position of potential well minima lie on the crystal nearest neighbour distances (first PDF peak position). As per Lucas et al.[2] and Rahman et al.[21] the dispersion terms were neglected for simplicity. The potential parameters were further refined by simulating the crystal structure at 500 K, which is below the melting point of the Zr/Ba/Na crystal, and comparing against the convoluted experimental PDFs. When no appreciable structural improvement could be made, the parameters were accepted. These potential parameters produced a simulation pressure of 4.15 $\pm$ 0.15 GPa at 300 K (*system B*)[26].

Reducing the pressure requires a reduction in the total potential energy of the system. This was achieved by reducing the F-F coulombic repulsion term, with the addition of an attractive 1/r term, to give a stable glass at 300 K. The pressure of this glass was atmospheric (0.09 $\pm$ 0.14 GPa) (*system A*). The potential parameters used are shown in tables 1 and 2.

The Zr/Ba/Na fluoride systems, A and B, contained 785 particles (114 Zr, 43 Ba, 43 Na and 585 F) within a cubic box of length 22.377 Å and were simulated by using FUNGUS, a molecular dynamics program [27, 28]. To avoid imposing any initial structure on the systems, all ions of the same type were placed adjacent to each other. The initial coordinates of each system corresponded to a NaCl structure of similar box size. The liquid was equilibrated at 6000 K for 3 ps NVT, (constant number of particles (N), constant volume (V) and constant temperature (T)), followed by 97 ps NVE, (constant number of particles (N), constant volume (V) and constant total energy (E)), using a time step of 1 fs. A variety of checks (e.g. monitoring pressure, total energy and homogeneity of the melt) were performed to

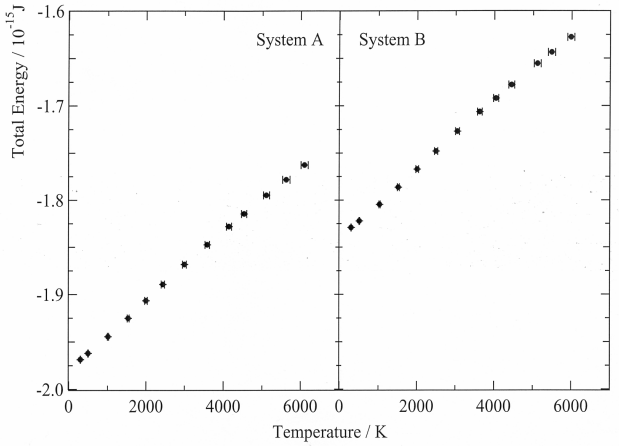

Figure 1. Variation of total energy versus temperature. *System A* is on the left and *system B* is on the right. These values have been averaged over 5 ps with the error bars being ± 1 SD and indicate the fluctuation in total energy and temperature.

ensure complete equilibration. The systems were then quenched in decrements of 500 K with 3 ps NVT and 17 ps NVE at each new temperature. Once 300 K was reached, 3 ps NVT and 37 ps NVE were performed to allow for structural relaxation [20]. Dynamic data was collected over the last 5 ps of each 10 ps run. Structural data was collected over the last 1 ps of each 10 ps run.

The coordinate file produced by each MD run was analysed by an output analysis program, FUNGO[29] to give the mean squared displacement (MSD) values. This file was also analysed by SPHERCOR, a program written by the author, to produce coordination and spherical average (see below) information. SPHERCOR required that the radial extent (or cut off) of the first coordinate sphere to be defined. This is normally taken to be the first minima after the first main PDF peak. With the exception of Zr-F, the first and higher coordinate spheres of the Zr/Ba/Na simulated glass pair distribution functions overlap making the selection of this point somewhat arbitrary and complicating the structural comparison.

The chemical homogeneity of the system was determined by an examination of the spherical average for each ion type, n_j, and the spherical average for all ions in the system, n_{all} [20]. In both cases, the radius used was half a simulation box length. The spherical average, n_j was computed using:

$$n_j(L/2) = \int_0^{L/2} \rho_j g_j(r) 4\pi r^2 dr \quad , \qquad (3)$$

where ρ_j is the density of ion type j, $g_j(r)$ is the pair distribution function of ion type j and L is the simulation box length. The spherical average of all ions in the system is computed from the addition of the n_j values for Ba-Ba, F-F, Na-Na and Zr-Zr. The expected value of n_j for a homogeneous distribution, n_j^*, is a fraction of the total number of ions of type j within the simulation box, N_j, minus the centre atom:

$$n_j^* = \frac{\pi N_j}{6} - 1 \quad . \qquad (4)$$

The expected value of n_{all} for a homogeneous distribution, n_{all}^*, was computed by summing the individual n_j^* values for each ion type. A fully equilibrated liquid, of uniform density, is expected to have values of n_j and n_{all} which are close to those for a homogeneous distribution (the exact value will depend on both the glass structure and the potentials used). However, the spherical average does not indicate the configurational variation since it is a self cancelling distribution (it is an average of both positive and negative values). Therefore the absolute deviation of the spherical average from homogeneity (referred to as the absolute deviation) was also calculated for each ion type:

$$n_j^{abs\_dev} = \frac{1}{no\_j\_ions} * \sum_{j\_ions} abs(nj - n_j^*) \quad , \qquad (5)$$

where no_j_ions is the number of ions of type j and j_ions represents each ion of type j. A value of close to, or, zero for the absolute deviations, $n_j^{abs\_dev}$ and $n_{all}^{abs\_dev}$, will only occur for a structure which is truly uniform on the scale of the spherical average radius.

3. Results

The dynamic data for both canonical ensemble simulations, *system A* and *system B* are indicated in Figures 1 to 3. All error bars are ± 1 standard deviation and are also indicative of the fluctuation in those points where the error bars are not shown. The errors in these simulations represent the uncertainty due to the fluctuations in thermodynamic and structural quantities observable on the time scale of these simulations and do not directly indicate, in anyway, the deviation of these quantities from their true liquid state values. In these figures, the results for *system A* are displayed on the left, while those for *system B* are displayed on the right. The total energy (figure 1) and pressure versus temperature curves (figure 2) are lowered by the reduction in pressure by about $1.4*10^{-16}$ J and 4 GPa respectively. All curves decrease almost linearly with temperature. The glass transition is indicated by a barely noticeable gradient decrease in the total energy and pressure curves between 2500 K and 1500 K (see derivative curves below). The pressure of *system A* at 300 K (0.09 GPa) is within one standard deviation of atmospheric pressure, 0.0001 GPa, and is statistically significantly different from that of *system B* (4.15 GPa). The magnitude of the uncertainty of the total energy and pressure curves also decrease with decreasing temperature. The final values,

Table 3. Pair distribution function (PDF) peak positions (nearest neighbour distances), average coordination numbers (CN) and cut off radii for the simulated Zr/Ba/Na systems (A and B) at 300 K. Experimental results for various compositions of Zr/Ba binary glasses are also presented [5, 33-38] . Note that X-ray or neutron scattering data for the Zr/Ba binary fluoride glass is difficult to interpret beyond the first two peaks (Zr-F, Ba-F) of the pair distribution function possibly resulting in greater errors for the experimental figures[49].

Ion Pair	PDF peak / nm			Average CN			Cut off Radii / nm	
	Simulation (±0.007) System		Experimental	Simulation (±0.04) System		Experimental	(±0.005) System	
	A	B		A	B		A	B
Ba-Ba	0.433	0.429	0.403-0.416	1.05	1.67		0.455	0.463
Ba-Na	0.409	0.427		1.17	0.92		0.450	0.450
Ba-F	0.262	0.261	0.26-0.28	6.95	7.05		0.310	0.310
Ba-Zr	0.433	0.438	0.403-0.416	6.61	6.11		0.470	0.470
Na-Na	0.348	0.333		1.29	1.67		0.380	0.380
Na-F	0.220	0.218		4.58	4.73		0.270	0.270
Na-Zr	0.378	0.381		4.83	4.72		0.430	0.430
F - F	0.252	0.252		6.12	6.09		0.300	0.300
Zr- F	0.197	0.198	0.206-0.27	6.87	6.90	6.0-8.0	0.230	0.230
Zr-Zr	0.409	0.408	0.403-0.416	4.14	4.15		0.450	0.450

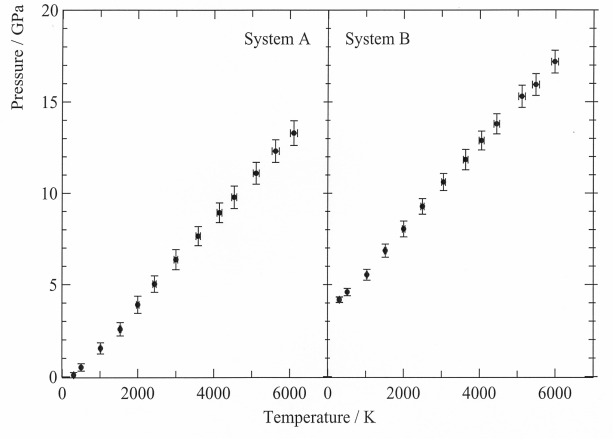

Figure 2. Pressure variation with temperature, averaged over 5 ps, of *system A* , left, and *system B* , right. The error bars represent ± 1 SD fluctuations for both pressure and temperature.

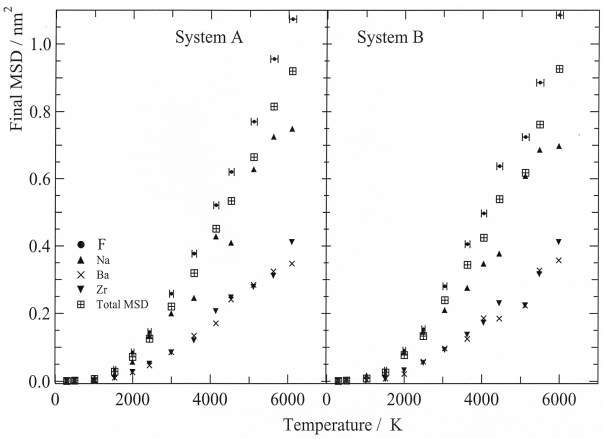

Figure 3. Variation of final mean square displacement after 5 ps versus temperature. The curve on the left is *system A* , with *system B* on the right. The total final mean square displacement is a weighted average of the four ions.

after an interval of 5 ps, of the mean squared displacement (MSD) are shown in figure 3 for both simulations. These curves are almost identical for both glasses and vary non-linearly, starting from a high initial value at 6000 K and decrease with decreasing temperature. An observable gradient change in the final MSD curves between 1500 K to 2500 K is also indicative of the glass transition. Fluoride, in both simulations, is the most mobile ion, with barium and zirconium being the least mobile with almost identical final MSD values. The final MSD values of sodium are closest to those of fluoride. The total final MSD values are also indicated in figure 3 for both simulations and represent the weighted average of all the ions.

The glass transition was examined in detail by using the derivative of pressure with respect to temperature (dP/dT); specific heat at constant volume, C_V (dE_{total}/dT); and the Arrhenius behaviour of the final values of MSD (ln(MSD) vs 1/T), figures 4 and 5. For clarity, only *system A* is shown in figure 5. The pressure derivatives for both glasses increase between 500 K and 2000 K, figure 4, showing that there is a broad transition in both systems. The specific heat, C_V (figure 4), increases between 300 K and 2000 K and the MSD departs from Arrhenius behaviour between 1000 K and 1500 K, figure 5, as a result of the glass transition. The high temperature region of figure 5 develops a concave downward curvature as is well known for these

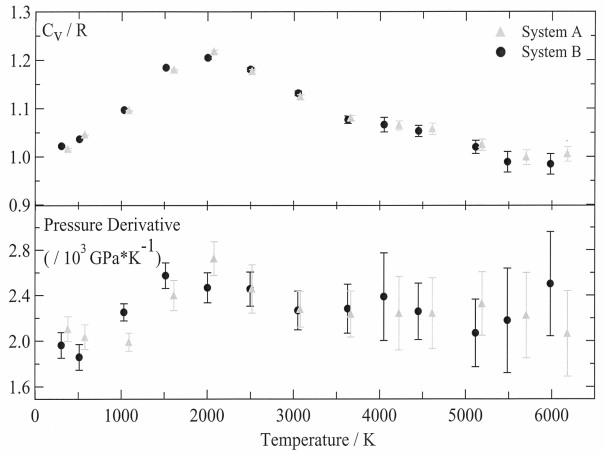

Figure 4. Derivates of total energy (C_V) and pressure, versus temperature, for both systems. For clarity the data points for *system A* have been offset by 80 K. The magnitude of the ± 1 standard deviation fluctuation of the gradients is also shown.

melts[30].

The structural changes during equilibration and cooling are observable in the spherical averages, an example of which is shown in figure 6. Displayed is the spherical average and the absolute deviation of the spherical average for *system A* (top) and *system B* (bottom). All the spherical averages have been normalised so that a homogeneous distribution has a value of one. In this figure, the absolute deviation of the spherical average has an offset of one so that it can be displayed on the same y-axis range as the spherical average. The errors in the spherical average, representing the structural changes due to diffusion processes, are also displayed and were obtained by analysing the structure over three consecutive 1 ps intervals. The ionic spherical averages have been examined in greater detail for selected points during both systems, figures 7 and 8. The n_j values for the crystal have also been included for comparison.

The PDFs were used to compare the structure of the two systems to experimental values in addition to verification of simulation consistency. Figure 9 displays the PDFs for *system A* . All the pair distribution functions were calculated to half a box length (1.12 nm) but, as there is only short range structure in glasses, are displayed only to 0.6 nm. The pair distribution functions range in width from the narrow, F-Zr and Zr-Zr, to moderate, Ba-Ba and Ba-Na. In all cases, the peaks have sharp features which are characteristic of the solid state. The position of the PDF peaks (nearest neighbour distances), coordination data and the cut offs used in calculating the structural data are summarised in table 3. Experimental data for Zr/Ba fluoride glass, where available, is also indicated in table 3. The results show that, in general, there is agreement between the nearest neighbour distances and coordination numbers for the experimental Zr/Ba and simulated Zr/Ba/Na fluoride glasses.

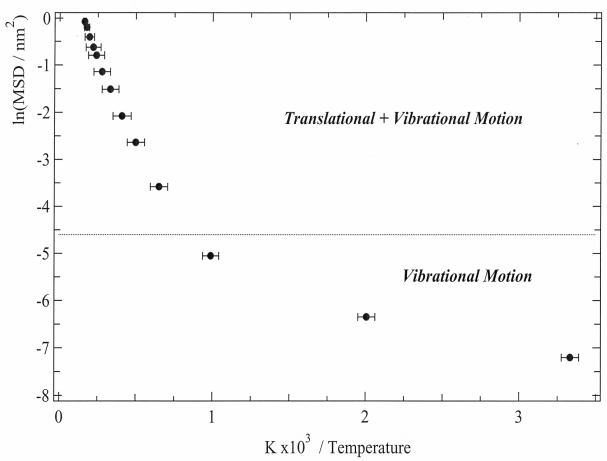

Figure 5. Arrhenius plot of the natural logarithm of the final mean squared displacement values after 5 ps against 1/T for *system A* . The error bars represent the ± 1 standard deviation fluctuations in temperature. The horizontal line at MSD ≈ 0.01 nm^2 indicates the distinction between long range diffusive motions and motions which, on the time scale of the simulation, correspond only to vibrations.

4. Discussion

Simulation consistency

The dynamic and static computational results, figures 1 to 3 and 6 to 9, show, [31], that at 300 K an equilibrated and homogeneous atmospheric pressure Zr/Ba/Na glass (within 1 SD) as well as a 4 GPa Zr/Ba/Na glass were successfully simulated using a physical density (*system A* and B respectively). At each temperature the dynamic quantities (pressure, total energy, potential energy and kinetic energy) oscillated about steady mean values without displaying any systematic drift, [32 p 171]. The final values of MSD (figure 3), n_{all} and n_j (figures 6 to 8), as well as the PDFs, also showed the same trends and confirmed structural equilibrium and homogeneity on the time scale of the simulation. Further validation of the successful simulation was given by a comparison (table 3) of cation-anion distances and Zr-F CN with previously reported structural experimental data for Zr/Ba fluoride glasses [5, 33-38]. The Zr/Ba fluoride glass was used as no experimental structural data was available for Zr/Ba/Na fluoride glass. This comparison is valid since the Zr/Ba based fluoride glasses are ionic with an anionic excess and the cation-anion distances will therefore remain essentially invariant under a changing composition. In addition, the range of the Zr-F CNs are also limited (6-8) by the high surface field strength of zirconium and the Zr:F radius ratio [24].

Potentials and pressure reduction

A stable, atmospheric pressure, NVT glass, *system A* , was achieved with a physical density at 300 K by decreasing the repulsive nature of the F-F coulombic interaction by 0.008 %. A reduction in the repulsive nature of the Zr-Zr potential resulted in barium and/or

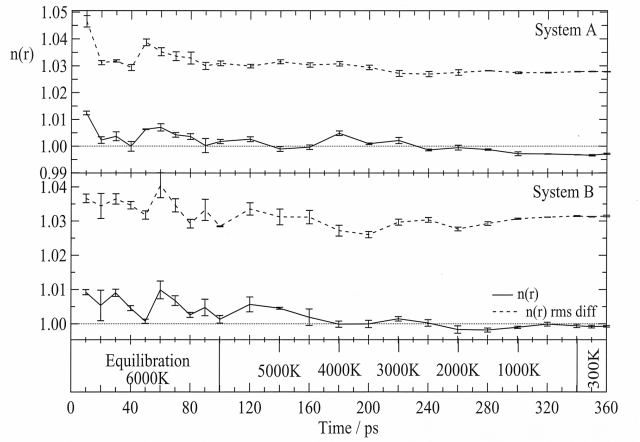

Figure 6. Variation of the spherical average and the absolute deviation of the spherical average from homogeneity for the total spherical average, n_{all}, versus time. Simulation temperatures are also indicated. The ± 1 SD error bars represent the structural variations due to vibrational and translation ionic motion.

sodium fluoride crystalline phases as did the reductions in the Ba-Ba, Ba-Na, Ba-Zr, Na-Na and Na-Zr repulsive potentials. Reducing the F-F exponential repulsive term did not lead to the required pressure reduction as the F-F potential is dominated by the coulombic term. It would be incorrect to interpret the reduction in the coulombic term as a reduction in the F ion charge; rather it should be seen as a result of limitations in the pair potential function used. Charge neutrality is nonetheless maintained [32]. The high coordination number of zirconium to fluoride would, most likely, accentuate three body interactions due to the presence of two strong (Zr F) and one weaker interaction (F-F). Hence, the need for this reduction is probably the result of significant higher order interactions[39].

The reduction in the F-F potential to achieve atmospheric pressure was difficult to achieve due to three interrelated factors. Firstly, the simulation pressure at 6000 K was found not to be directly related to the simulation pressure at 300 K. This was caused by the pressure versus temperature curve being non-linear around the glass transition region (discussed further below) with the pressure gradient change dependant on the potential used. Secondly, as the pressure versus F-F potential repulsion curve has a reversed 's' shape, with the greatest slope being at 0 atmospheres, step changes in the F-F repulsive potential resulted in an increasing pressure change. Therefore, finding the correct F-F potential reduction was an iterative process. Thirdly, the pressure was very sensitive to a very small change in the F-F repulsive potential making prediction of the correct F-F potential reduction even more difficult. For example, a 0.00004 % change in the F-F potential causes a large, ≈ 0.4 GPa, change in pressure.

Despite using the Zr/Ba/Na fluoride crystal structure to tune the pair potentials, no similarities in the spherical average were shown between the crystal and the equilibrated liquid or glass, nor was any medium or long range order introduced into the glass. The spherical average n_j values for both the crystal and the starting configuration differ markedly from homogeneity, figures 7 and 8. However, after equilibration at 6000 K and in the 300 K glass, the n_j values are very close to a homogeneous value. Additionally, in contrast to the Zr/Ba/Na fluoride crystal, the PDFs for the equilibrated liquid and glass all reach an average value of one for g(r) within a distance of 0.6 nm from any central ion with no distinct features at greater distances. Computer 3D modelling of the equilibrated and glass structures did not show any medium or long range order. However, as expected, similarities were shown in these simulations between the crystal and the glasses in their short range order [24, 25, 40].

Glass transition

The change in gradient close to 1500 K of the MSD curve, figure 3 and the pressure curve, figure 2 , can be attributed to the glass transition. It is well known that the thermal expansion coefficient, $\alpha = (1/V)(\partial V/\partial T)_P$, measured at constant pressure, has a discontinuity at the glass transition and increases in magnitude on further heating in most systems [30, 41, 42]. Similarly, the compressibility, $\kappa = (-)(1/V)(\partial V/\partial P)_T$, also has a discontinuity at T_g and increases in magnitude above the glass transition temperature[30, 41, 43]. The thermal expansion, compressibility and pressure gradient are related by the following thermodynamical relationship:

$$(\frac{\partial P}{\partial T})_V = \frac{\alpha}{\kappa} \quad . \qquad (6)$$

Therefore, the pressure derivative in a constant volume simulation is expected to show a discontinuity at the glass transition, as observed in figure 4 for both systems. This discontinuity is, however, more gradual for *system B* showing that the higher value of F-F repulsion acts as an inhibitor to structural reconfiguration.

The onset of the glass transition can be found by the region of non-Arrhenius behaviour in MSD, occurring between 1000 K and 1500 K for both glasses, figure 5, as compared with 514 K for a fluoride glass of similar composition (59.9 mole % ZrF_4: 20 BaF_2: 20 NaF_2: 0.1 InF_3) [5]. At high temperatures the atomic motion is dominated by the translational component. Arrhenius behaviour is shown in this region , [44 p 518], with the calculated activation energy for diffusion, 62 kJ/mole, in the atmospheric pressure simulation comparing favourably with the experimental viscous flow activation energy for $BaZr_2F_{10}$, 67.4 kJ/mole, at 873 K (viscosity vs. T^{-1} curves in [45] show that the activation energies for $BaZr_2F_{10}$ and $NaBa_3Zr_6F_{31}$ glasses are similar) [45 (tabulated data)]. Therefore, the activation energy does not vary greatly in the liquid region which is in agreement with experimental data [45, 46]. Subsequently, during cooling of the liquid, the translational motion decreases and, when it approaches values around an atomic radius, the MSD curve deviates

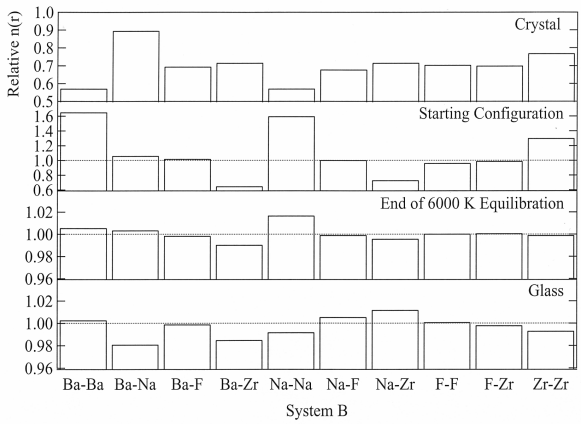

Figure 7. Spherical averages of each ion pair, n_j, at selected temperatures during *system B* . All values have been adjusted so that a value of one represents a homogenous distribution. Different y scaling was used for each temperature to display the differences between n_j values.

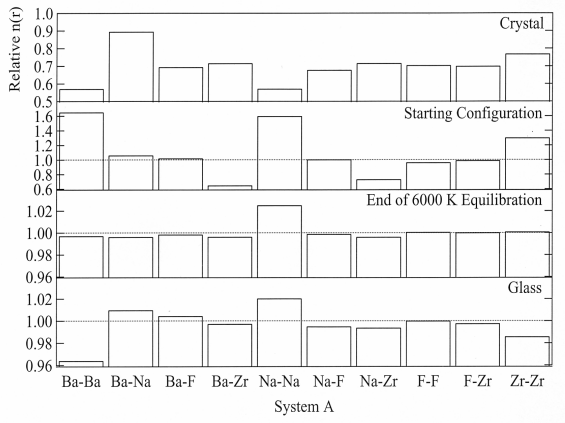

Figure 8. Spherical average of each ion pair, n_j, at selected temperatures during *system A* . All values have been adjusted so that a value of one represents a homogenous distribution. Different y scaling was used for each temperature to display the differences between n_j values.

from Arrhenius behaviour.

The simulated glass transition occurs at a higher temperature than the experimental value due to the simulation cooling rate, $-2.4*10^{13}$ K/sec, being much greater than even very fast splat quenching, -10^7 K/sec. It is this very high cooling rate which causes the temperature at which the liquid equilibration rate is slower than its cooling rate (i.e. the glass transition) to be very high[8]. Broader simulated glass transitions are also caused by the high glass transition temperature. The relaxation rate towards a metastable liquid equilibrium during the glass transition changes by at least two orders of magnitude. However, at high temperatures, the relaxation rate varies slowly with temperature and therefore the glass transition occurs over a broad temperature range [13].

The glass transition in the Zr/Ba/Na fluoride glass is caused by the breaking up of structural and geometric constraints in the glass. At room temperature the specific heat, figure 4, is close to 3R, with all the vibrational energy levels excited and therefore a full complement of vibrational modes. On heating, the excitation of translational energy levels and the subsequent change of the vibrational spectrum, causes a peaking (the magnitude is ≈ 0.6R) in the specific heat which is of the same magnitude and shape as that predicted by Angell's 'Bond Lattice model'[47, 48]. In this model it is the breaking of discrete bonds that causes the peaking of specific heat; however it is suggested here that a parallel can be made with the breaking up of structural geometric constraints in the simulated glass.

Structural equilibration

The approach to structural equilibrium at high temperatures was monitored by examining the spherical averages. The initial configurations for both *systems A* and *B* have spherical averages, (figures 6 to 8) that deviate significantly from homogeneity. During equilibration at 6000 K, the spherical averages tended towards a homogeneous value. At the termination of equilibration, the spherical averages were close to a homogenous value and showed no artefacts of the starting configuration or of the Zr/Ba/Na crystal, figures 7 and 8. Therefore, the tendency of the spherical averages to reach a steady state value at constant temperature can be used as an indication of structural equilibration.

The onset of the glass transition could also be observed using the spherical average. During cooling, the gradient of the spherical averages decreased and approached zero, indicating that the structures within the melt were being 'locked in'. At the glass transition temperature the spherical averages plateau. Therefore, the plateauing of the spherical averages during cooling indicates the onset of the glass transition

The configurational variations occurring during the simulations of *systems A and B* were examined by using the absolute deviation, figure 6. The absolute deviation showed very similar behaviour to the spherical average with a plateau in the absolute deviation indicating either structural equilibration at constant temperature or, a 'locking in' of structures during cooling. The decrease in the absolute deviation during cooling indicates that the simulation was no longer able to explore all the configurations available to the liquid. Thus, the absolute deviation can be used to show the structural variation occurring during the simulation as well as a further pointer to structural equilibrium and the onset of the glass transition.

Confirmation of the homogeneity and stability of the glasses for both systems at 300 K was given by the value of the spherical averages. The spherical average values for each ion pair (n_j) for both systems, figures 7 and 8, were close to homogeneous confirming the amorphous nature of the glasses. The values of the spherical average also indicated that the quantity of crystalline phases, if present, were insignificant and therefore that the systems

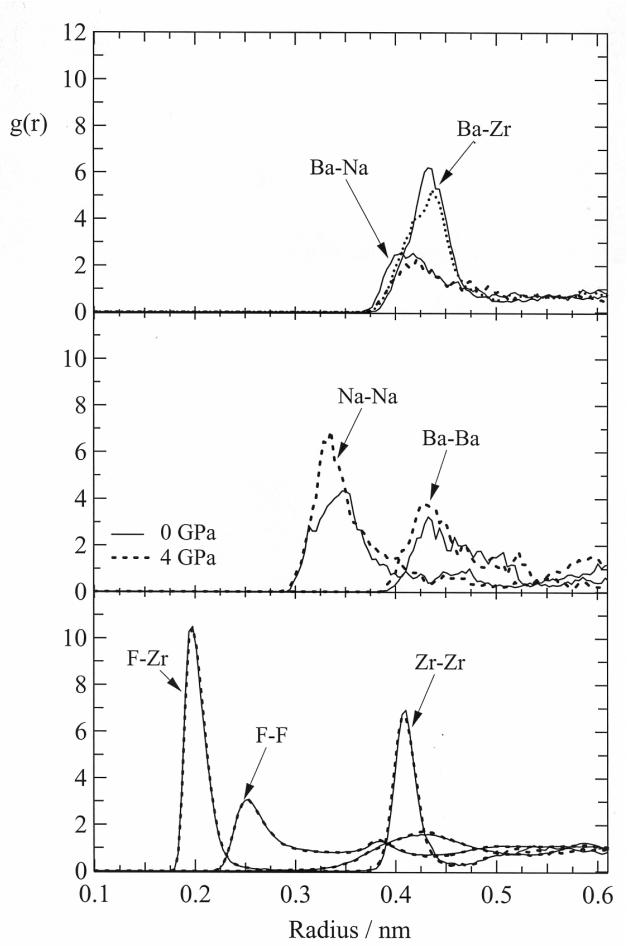

Figure 9. Pair distribution functions for the atmospheric pressure Zr/Ba/Na glass at 300 K (*System A*).

were stable. Hence, the spherical averages are a simple test that can be used to indicate the particle distribution as well as the stability of the simulation.

The spherical averages also reflected the altering of the dynamics of the simulation with the reduction in pressure. Reaching homogeneity 10 ps earlier, the spherical average for *system A* , figure 6, shows that it has a greater structural relaxation rate than *system B*. *System A* also remains closer to homogeneity during cooling, with the average structural variation, (shown by the absolute deviation), lower than for *system B* . Both these changes have been brought on by the lowering of the energy barrier to structural reconfiguration as a result of the reduction in the fluoride-fluoride repulsion.

5. Conclusion

An atmospheric pressure structure of Zr/Ba/Na fluoride glass at 300 K has been successfully simulated by canonical molecular dynamics. The decrease in pressure, compared to previous work, was achieved by the reduction of the F-F repulsion to account for significant three body and higher order ion-ion interactions. Although both the structural and thermodynamic properties were affected by the potential change, no change in the diffusion rate was observable.

Tuning the pair potentials against a Zr/Ba/Na fluoride crystal structure provided the means by which a Zr/Ba/Na fluoride glass, lacking experimental structural data, could be simulated. Both the equilibrated melts and 300 K glasses show no medium and long range structural evidence of crystalline phases as well as no structural evidence of the starting configuration. However, as expected, there are similarities in the short range order between the glass and crystal structures. In addition, the bond lengths obtained in the atmospheric pressure glass at 300 K compare favourably with previously reported experimental data for Zr/Ba fluoride glasses (no experimental structural data was available for Zr/Ba/Na fluoride glasses).

Both simulations show a broad glass transition occurring in the region 1500-2000 K. The glass transition is evident in a number of properties including MSD, C_V and the absolute deviation in n(r). The specific heat shows a peaking at the glass transition, i.e. at the onset of translational motion, that is of the same magnitude and shape as that predicted by Angell's 'Bond Lattice' model. It is therefore suggested that the glass transition is the temperature at which the breaking up of structural geometric constraints in the simulated glass occurs.

Changes in the structure during the simulation as well as an indication of the equilibration can be obtained by monitoring the ion-ion spherical averages as well as its standard deviation. A levelling of the spherical averages, along with the reduction in its standard deviation, can also be used as additional indicators of the glass transition.

Acknowledgments

The use of the Monash University Computer Centres SGI 'supercomputer' is gratefully acknowledged.

References

1. C A Angell, P A Cheesemann and S Tamaddon, *Journal de Physique* C9, **43,** 12 (1982) 291-301.
2. J Lucas, C A Angell and S Tamaddon, *Mat. Res. Bull*, **19** (1984) 945-951.
3. Y Kawamoto, et al., *J. Chem. Phys.*, **83,** 5 (1985) 2398-2404.
4. B Boulard, et al., *Mat. Sci. Forum*, **32-33** (1988) 61-68.
5. A Uhlherr, et al., *Mat. Sci. Forum*, **67 & 68** (1991) 431-436.
6. C A Angell, *Pure and Applied Chemistry,* **63** (1991) 1387-1392.
7. C A Angell, D R MacFarlane and M Oguni, *The Kauzmann Paradox, Metastable Liquids, and Ideal Glasses - A summary.* Annals New York Academy of Science, **484** (1987) 241-247.
8. C A Angell, *Chem. Rev.*, **90** (1990) 523-542.

9. L V Woodcock, C A Angell and P Cheeseman, *J. Chem. Phys*., **65**, 4 (1976) 1565-1577.
10. C A Angell, J H R Clarke and L V Woodcock, *Advances in Chemical Physics*, I Prigogine and S A Rice, Editors (1981).
11. J P Hansen, *Physica A,* **201** (1993) 138-149.
12. S L Shumway, A S Clarke and H Jonsson, *J. of Chem. Phys*., **102**, 4 (1995) 1796-1805.
13. C A Angell and L M Torell, J. *of Chem. Phys.*, **78**, 2 (1983) 937-945.
14. R G D Valle and H C Andersen, *J. of Chem. Phys.*, **97**, 4 (1992) 2682-2689.
15. S R Kudchadkar and J M Wiest, *J. of Chem. Phys.,* **103**, 19 (1995) 8566-8576.
16. K L Ngai, C M Roland and G N Greaves, *J. of Non-Cryst. Solids,* **182** (1995) 172-179.
17. F Sciortino, et al., *Phys. Rev. E,* **54**, 6 (1996) 6331-6343.
18. K Kinugawa, *J. of Chem. Phys.*,**97**,11 (1992). 8581-8595.
19. Kinugawa, K, *Glass Research at ONRI 1993*. Osaka National Research Institute (1994) 154-166.
20. S Gruenhut, et al., *Molecular Simulation*, **19** (1997) 139-160.
21. A Rahman, R H Fowler and A H Narten, *J. Chem. Phys.,* **57**, 7 (1972) 3010-3011.
22. S Gruenhut and D R MacFarlane, *J. Non-cryst. Solids,* **184** (1995) 356-362.
23. J P Laval and A Abaouz, *J. of Solid State Chem.,* **101 (**1992) 18-25.
24. M Poulain, *Glass systems and structures*, in *Fluoride Glasses*, A E Comyns, Editor. John Wiley & Sons: Cichester (1989)11-48.
25. K H Sun, *Journal of the American Ceramic Society,* **30** (1947) 277.
26. S Gruenhut, et al., *J. of Non-Cryst. Solids,* **213&214** (1997) 398-403.
27. J R Walker, *Molecular Dynamics Simulations of Crystalline Ionic Materials*, in *Computer Simulation of Solids*, C R A Catlow and W C Mackrodt, Editors, Springer-Verlag. (1982) 58-66.
28. *Catalysis User Guide 2.3.0*. 1993, San Diego, USA: Biosym Technologies.
29. G E Mills, *FUNGO* 1995: Biosym Technologies.
30. C A Angell, . *J. of Non-Cryst. Solids*, **102** (1988) 205-221.
31. S Gruenhut, PhD *Thesis,* Dept. of *Chemistry*. Monash University: Melbourne, Australia (1998).
32. M P Allen and D J Tildesley, *Computer Simulation of Liquids*, Oxford University Press (1990).
33. R M Almeida and J D Mackenzie, *J. Chem. Phys.*, **74**, 11 (1981) 5954-5961.
34. S H Ko and R H Doremus, *Phys. Chem. Glasses,* **32**, 5 (1991) 196-201.
35. C N J Wagner, et al., *Mat. Sci. Forum,* **19-20** (1987) 137-140.
36. Y Kawamoto and T Horisaka, *J. Non-Cryst. Solids,* **56** (1983) 39-44.
37. W C Wang, Y Chen and T D Hu, *Phys. Stat. Sol. A* **136** (1993) 301-310.
38. R Coupe, et al., *J. of Am. Ceramics Soc.,* **66**, 7 (1983) 523-529.
39. B Vessal, *Personal Communication* (1995).
40. S Gruenhut, et al., *J. Chem Phys.* (1998).
41. W Kauzmann, , *Chemical Reviews,* **43** (1948) 219-256.
42. L D Landau and E M Lifshitz, *Statistical Physics Part 1*. 3'rd ed. Course of Theoretical Physics. Vol. 5. Oxford: Peragom Press(1998).
43. D R Lide, ed. *Handbook of Chemistry and Physics*. 74th ed. 1993 - 1994, CRC Press: Boca Raton.
44. C Kittel, *Introduction to Solid State Physics*. 6'th ed. 1986, NewYork: John Wiley and Sons, Inc.
45. H Hu and J D MacKenzie, *Journal of Non-Crystalline Solids,* **54** (1983) 241-251.
46. C A Angell, *Journal of Non-Crystalline Solids,* **131-133** (1991) 13-31.
47. C A Angell, *Journal of Physical Chemistry,* **75**, 24 (1971) 3698-3705.
48. K J Rao and C A Angell, *Thermodynamic and Relaxational aspects of the Glass Transition from a 'Bond Lattice' Model*, in *Amorphous Materials*, R W Douglas and B Ellis, Editors. Wiley-Interscience London(1972) 170-181.
49. C A Angell and C C Phifer, *Mat. Sci. Forum,* **32-33** (1988) 373-384.